J|A|C|S ARTICLES

Published on Web 04/13/2010

Time Averaging of NMR Chemical Shifts in the MLF Peptide in the Solid State

Itzam De Gortari,[†] Guillem Portella,[‡,||] Xavier Salvatella,[§,¶] Vikram S. Bajaj,[⊥,×] Patrick C. A. van der Wel,[⊥,⊗] Jonathan R. Yates,[†,#] Matthew D. Segall,[†] Chris J. Pickard,[†,+] Mike C. Payne,[†] and Michele Vendruscolo*[,§]

TCM Group, Cavendish Laboratory, University of Cambridge, Madingley Road, Cambridge CB3 0HE, United Kingdom, Computational Biomolecular Dynamics Group, Max-Planck-Institute for Biophysical Chemistry, Am Fassberg 11, 37077 Göttingen, Germany, Department of Chemistry, University of Cambridge, Lensfield Road, Cambridge CB2 1EW, United Kingdom, and Department of Chemistry, Francis Bitter Magnet Laboratory, Massachusetts Institute of Technology, Boston Massachusetts 02139

Received July 26, 2009; E-mail: mv245@cam.ac.uk

Abstract: Since experimental measurements of NMR chemical shifts provide time and ensemble averaged values, we investigated how these effects should be included when chemical shifts are computed using density functional theory (DFT). We measured the chemical shifts of the *N*-formyl-L-methionyl-L-leucyl-L-phenylalanine-OMe (MLF) peptide in the solid state, and then used the X-ray structure to calculate the ^{13}C chemical shifts using the gauge including projector augmented wave (GIPAW) method, which accounts for the periodic nature of the crystal structure, obtaining an overall accuracy of 4.2 ppm. In order to understand the origin of the difference between experimental and calculated chemical shifts, we carried out first-principles molecular dynamics simulations to characterize the molecular motion of the MLF peptide on the picosecond time scale. We found that ^{13}C chemical shifts experience very rapid fluctuations of more than 20 ppm that are averaged out over less than 200 fs. Taking account of these fluctuations in the calculation of the chemical shifts resulted in an accuracy of 3.3 ppm. To investigate the effects of averaging over longer time scales we sampled the rotameric states populated by the MLF peptides in the solid state by performing a total of 5 μs classical molecular dynamics simulations. By averaging the chemical shifts over these rotameric states, we increased the accuracy of the chemical shift calculations to 3.0 ppm, with less than 1 ppm error in 10 out of 22 cases. These results suggests that better DFT-based predictions of chemical shifts of peptides and proteins will be achieved by developing improved computational strategies capable of taking into account the averaging process up to the millisecond time scale on which the chemical shift measurements report.

Introduction

As NMR chemical shifts are uniquely sensitive probes of the chemical environment of atoms they are, at least in principle, tk;2particularly well suited for characterizing the structure and the dynamics of proteins.[1−3] Since these NMR observables can be measured readily and with great accuracy there is a great interest in the development of procedures to exploit the information provided by chemical shifts for protein structure determination.[4−10] If the relationship between chemical shifts and protein structures could be understood in better detail, in the longer term it might become possible to address cases that pose significant challenges for traditional methods of structure determination, and for which chemical shifts are often the only observables that can be measured with any degree of completeness; these systems include proteins and protein complexes of

[†] Cavendish Laboratory, University of Cambridge.
[‡] Max-Planck-Institute for Biophysical Chemistry.
[§] Department of Chemistry, University of Cambridge.
[⊥] Massachusetts Institute of Technology.
[||] Institute for Research in Biomedicine, Baldiri Reixac 10-12, 08028 Barcelona, Spain.
[¶] ICREA and Institute for Research in Biomedicine, Baldiri Reixac 10-12, 08028 Barcelona, Spain.
[#] Department of Materials, University of Oxford, Parks Road, Oxford, OX1 3PH, UK.
[+] Department of Physics & Astronomy, University College London, Gower St, London, WC1E 6BT, UK.
[×] Materials Sciences Division, Lawrence Berkeley National Laboratory and Department of Chemistry, University of California, Berkeley, Berkeley, CA.
[⊗] University of Pittsburgh, Department of Structural Biology, Pittsburgh, PA 15260.

(1) Szilagyi, L. *Prog. Nucl. Magn. Reson. Spectrosc.* **1995**, *27*, 325–443.
(2) Wishart, D. S.; Case, D. A. *Methods Enzym.* **2001**, *338*, 3–34.
(3) Oldfield, E. *Annu. Rev. Phys. Chem.* **2002**, *53*, 349–378.
(4) Cavalli, A.; Salvatella, X.; Dobson, C. M.; Vendruscolo, M. *Proc. Natl. Acad. Sci. U.S.A.* **2007**, *104*, 9615–9620.
(5) Shen, Y.; et al. *Proc. Natl. Acad. Sci. U.S.A.* **2008**, *105*, 4685–4690.
(6) Wishart, D. S.; Arndt, D.; Berjanskii, M.; Tang, P.; Zhou, J.; Lin, G. *Nucleic Acids Res.* **2008**, *36*, W496–W502.
(7) Montalvao, R.; Cavalli, A.; Salvatella, X.; Blundell, T. L.; Vendruscolo, M. *J. Am. Chem. Soc.* **2008**, *130*, 15990–15996.
(8) Robustelli, P.; Cavalli, A.; Vendruscolo, M. *Structure* **2008**, *16*, 1764–1769.
(9) Shen, Y.; Vernon, R.; Baker, D.; Bax, A. *J. Biomol. NMR* **2009**, *43*, 63–78.
(10) Das, R.; Andre, I.; Shen, Y.; Wu, Y.; Lemak, A.; Bansal, S.; Arrowsmith, C. H.; Szyperski, T.; Baker, D. *Proc. Natl. Acad. Sci. U.S.A.* **2009**, *106*, 18978–18983.

large molecular weight,[11,12] amyloid fibrils,[13−16] membrane proteins,[17,18] and non-native intermediate states.[19]

A major role in the development of quantitative methods to use chemical shifts in structural biology is played by *ab initio* methods, which provide a detailed characterization of the variety of factors that influence the chemical shifts and their accurate computation from molecular structures. These calculations have been used to study the structure of proteins in the last 20 years and have been shown to have significant potential for structure determination.[20−32]

One aspect that can complicate the comparison between calculated and experimental chemical shifts is that the latter represent ensemble and time averages, whereas theoretical calculations are most readily performed by considering just one particular configuration of the system at a given time. Since peptides and proteins undergo significant structural fluctuations at biologically relevant temperatures, it is expected that their instantaneous chemical shifts will also fluctuate significantly. The effects of conformational averaging, as well as those due to the presence of the periodicity of the solid-phase environment, have been investigated in the literature for a variety of systems.[33−44] In particular, the introduction of a method capable of describing the bulk behavior of condensed phases through the use of periodic boundary conditions has recently enabled the analysis of the effects of conformational averaging on proton chemical shifts of ice and liquid water[45] by extracting conformations from trajectories generated by the Car−Parrinello molecular dynamics simulations. This type of study has been extended by, among others, Sebastiani and Parrinello,[46] who reported fluctuations up to 10 ppm for proton chemical shifts in water, and more recently by Dumez and Pickard,[43] who showed that motional averaging is an essential component of chemical shift calculations in organic solids.

In this work, we present a comparison of experimental measurements of chemical shifts with the results of molecular dynamics simulations combined with NMR chemical shift calculations with a treatment of the periodic boundary conditions for the *N*-formyl-L-methionyl-L-leucyl-L-phenylalanine-OMe (MLF) peptide in the crystal state.[47] The MLF peptide is a system that is very well characterized experimentally as it has been used to develop solid-state NMR techniques.[48−50] In order to assess the influence of structural fluctuations on the chemical shielding parameters in the MLF crystal, we considered an ensemble of configurations extracted from a 2 ps first-principles molecular dynamics simulation, together with another ensemble of configurations derived from 5 μs classical molecular dynamics simulations. Our results indicate that a promising approach to predict chemical shifts in peptides and proteins is to use a combination of classical molecular dynamics simulations and DFT calculations in order to take into account the configurational averaging that takes place over the chemical shift time scale.

Methods

NMR Measurements. Unlabeled MLF peptides (Bachem; Torrance, CA) were crystallized by slow evaporation from benzene, according to the procedure reported by Gavuzzo et al.[47] The resulting crystals were dried *in vacuo* and packed into a 4 mm MAS rotor (Varian Inc., Fort Collins, CO). One-dimensional (1D) ^{13}C and ^{15}N CP spectra were obtained using home-built spectrometers operating at 500 and 380 MHz ^{1}H frequencies (courtesy of D.J. Ruben, Francis Bitter Magnet Laboratory, MIT). Measurements were done at room temperature, using triple channel ($^{1}H/^{13}C/^{15}N$) probes and an 8−10 kHz MAS rate.[50] The ^{13}C and ^{15}N chemical shifts were referenced to dilute aqueous 2,2-dimethyl-2-silapentane-5-sulfonic acid (DSS) and liquid NH_3, respectively, via external and indirect referencing using the adamantane ^{13}C signals.[51−53] Since the peptide was unlabeled, no 2D assignment experiments were performed. Table 2 lists the measured chemical shifts along

(11) Fiaux, J.; Bertelsen, E. B.; Horwich, A. L.; Wuthrich, K. *Nature* **2002**, *418*, 207–211.
(12) Kay, L. E. *J. Magn. Reson.* **2005**, *173*, 193–207.
(13) Jaroniec, C. P.; MacPhee, C. E.; Bajaj, V. S.; McMahon, M. T.; Dobson, C. M.; Griffin, R. G. *Proc. Natl. Acad. Sci. U.S.A.* **2004**, *101*, 711–716.
(14) Tycko, R. *Curr. Opin. Struct. Biol.* **2004**, *14*, 96–103.
(15) van der Wel, P. C. A.; Lewandowski, J. R.; Griffin, R. G. *J. Am. Chem. Soc.* **2007**, *129*, 5117–5130.
(16) Wasmer, C.; Lange, A.; Van Melckebeke, H.; Siemer, A. B.; Riek, R.; Meier, B. H. *Science* **2008**, *319*, 1523–1526.
(17) Fernandez, C.; Hilty, C.; Wider, G.; Guntert, P.; Wuthrich, K. *J. Mol. Biol.* **2004**, *336*, 1211–1221.
(18) Hwang, P. M.; Bishop, R. E.; Kay, L. E. *Proc. Natl. Acad. Sci. U.S.A.* **2004**, *101*, 9618–9623.
(19) Vallurupalli, P.; Hansen, D. F.; Kay, L. E. *Proc. Natl. Acad. Sci. U.S.A.* **2008**, *105*, 11766–11771.
(20) Ditchfield, R. *Mol. Phys.* **1974**, *27*, 789–807.
(21) de Dios, A. C.; Oldfield, E. *J. Am. Chem. Soc.* **1994**, *116*, 11485–11488.
(22) Cheeseman, J. R.; Trucks, G. W.; Keith, T. A.; Frisch, M. J. *J. Chem. Phys.* **1996**, *104*, 5497–5509.
(23) de Dios, A. C. *Prog. Nucl. Magn. Reson. Spectrosc.* **1996**, *29*, 229–278.
(24) Havlin, R. H.; Le, H. B.; Laws, D. D.; de Dios, A. C.; Oldfield, E. *J. Am. Chem. Soc.* **1997**, *119*, 11951–11958.
(25) Helgaker, T.; Jaszunski, M.; Ruud, K. *Chem. Rev.* **1999**, *99*, 293–352.
(26) Cai, L.; Fushman, D.; Kosov, D. S. *J. Biomol. NMR* **2008**, *41*, 77–88.
(27) Cai, L.; Fushman, D.; Kosov, D. S. *J. Biomol. NMR* **2008**, *43*, 245–253.
(28) Casabianca, L. B.; De Dios, A. C. *J. Chem. Phys.* **2008**, *128*, 052201.
(29) De Gortari, I.; Galvan, M.; Ireta, J.; Segall, M.; Pickard, C. J.; Payne, M. *J. Phys. Chem. A* **2007**, *111*, 13099–13105.
(30) Thonhauser, T.; Ceresoli, D.; Mostofi, A. A.; Marzari, N.; Resta, R.; Vanderbilt, D. *J. Chem. Phys.* **2009**, *131*, 101101.
(31) Thonhauser, T.; Ceresoli, D.; Marzari, N. *Int. J. Quantum Chem.* **2009**, *109*, 3336–3342.
(32) Giannozzi, P.; et al. *J. Phys.: Condens. Matter* **2009**, *21*, 395502.
(33) de Dios, A. C.; Pearson, J. G.; Oldfield, E. *Science* **1993**, *260*, 1491–1496.
(34) de Dios, A. C.; Laws, D. D.; Oldfield, E. *J. Am. Chem. Soc.* **1994**, *116*, 7784–7786.
(35) Vila, J. A.; Baldoni, H. A.; Ripoll, D. R.; Scheraga, H. A. *J. Biomol. NMR* **2003**, *26*, 113–130.
(36) Svishchev, I. M.; Kusalik, P. G. *J. Am. Chem. Soc.* **2003**, *115*, 8270–8272.
(37) Bühl, M.; Mauschick, F. T. *Phys. Chem. Chem. Phys.* **2002**, *4*, 5508–5514.
(38) Nowakowski, J.; Miller, J. L.; Kollman, P. A.; Tinoco, J. *J. Am. Chem. Soc.* **1996**, *118*, 12812–12820.
(39) Piana, S.; Sebastiani, D.; Carloni, P.; Parrinello, M. *J. Am. Chem. Soc.* **2001**, *123*, 8730–8737.
(40) Komin, S.; Gossens, C.; Tavernelli, I.; Rothlisberger, U.; Sebastiani, D. *J. Phys. Chem. B* **2007**, *111*, 5225–5232.
(41) d'Avezac, M, M.; Marzari, N.; Mauri, F. *Phys. Rev. B* **2008**, *76*, 165122.
(42) Cadars, S.; Lesage, A.; Pickard, C. J.; Sautet, P.; Emsley, L. *J. Phys. Chem. A* **2009**, *113*, 902–911.
(43) Dumez, J. N.; Pickard, C. J. *J. Chem. Phys.* **2009**, *130*, 104701.
(44) Gervais, C.; Bonhomme-Coury, L.; Mauri, F.; Babonneau, F.; Bonhomme, C. *Phys. Chem. Chem. Phys.* **2009**, *32*, 6953–6961.
(45) Pfrommer, B. G.; Mauri, F.; Louie, S. G. *J. Am. Chem. Soc.* **2000**, *122*, 123–129.
(46) Sebastiani, D.; Parrinello, M. *ChemPhysChem* **2002**, *3*, 675–679.
(47) Gavuzzo, E.; Mazza, F.; Pochetti, G.; Scatturin, A. *Int. J. Pept. Protein Res* **1989**, *34*, 409–415.
(48) Rienstra, C. M.; Hohwy, M.; Mueller, L. J.; Jaroniec, C. P.; Reif, B.; Griffin, R. G. *J. Am. Chem. Soc.* **2002**, *124*, 11908–11922.
(49) Jaroniec, C. P.; Filip, C.; Griffin, R. G. *J. Am. Chem. Soc.* **2002**, *124*, 10728–10742.
(50) Bajaj, V. S.; van der Wel, P. C. A.; Griffin, R. G. *J. Am. Chem. Soc.* **2009**, *131*, 118–128.

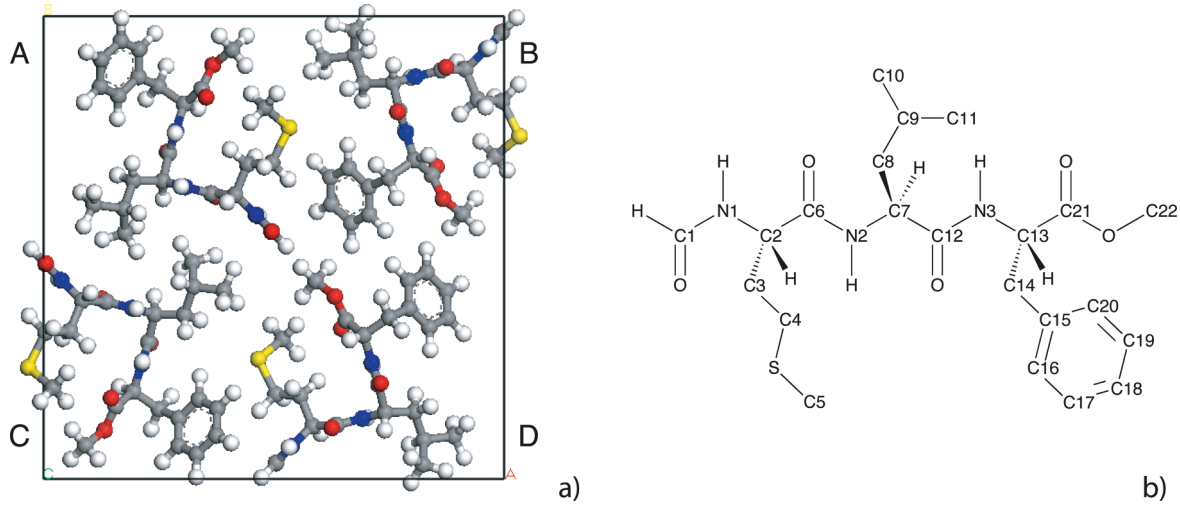

Figure 1. (a) *N*-Formyl-L-methionyl-L-leucyl-L-phenylalanine-OMe (MLF) unit cell, comprising four molecules. (b) Schematic representation of the MLF peptide.

with their likely assignments based on analogy with previous measurements on the closely related *N*-formyl-Met-Leu-Phe-OH peptide.[48,54]

First-Principles Calculations. All electronic structure calculations were performed within the plane wave-pseudopotential implementation of density functional theory (DFT)[55] and use the Perdew−Burke−Ernzerhof (PBE) generalized gradient approximation to exchange and correlation terms.[56] This exchange-correlation potential allows an accurate evaluation of the NMR parameters to be made.[57]

Geometry Optimization. As a starting point for the calculations, we considered a crystal structure of the MLF peptide[47] (CDS Refcode: SEYJEL, Figure 1). MLF crystallizes in the orthorhombic system space group $P2_12_12_1$, with unit-cell parameters: a = 21.727 Å, b = 21.836 Å, c = 5.133Å, Z = 4. As the positions of hydrogen atoms reported by X-ray diffraction are considerably less accurate than the corresponding positions of heavy atoms, we performed a partial geometry optimization, allowing only the position of the hydrogen atoms to move; we used the CASTEP code,[58,59] keeping the heavy nuclei fixed and allowing the hydrogen atoms to relax. The calculations used ultrasoft pseudopotentials,[60] and the basis set included plane waves up to a maximum energy of 29 Ry with one k-point (1/4,1/4,1/4). The energy tolerance was set to 1×10^{-5} eV.

First-Principles Molecular Dynamics Simulations. First-principles molecular dynamics simulations were carried out using the CASTEP code.[58,59] For the geometry optimization calculations we used the ultrasoft pseudopotentials[60] and a basis set that included plane waves up to a maximum energy of 29 Ry with one k-point, (1/4,1/4,1/4). In the molecular dynamics simulations we used the velocity Verlet algorithm for integration of the equation of motion. Electrons were kept on the Born−Oppenheimer surface by means of explicit electronic minimization after each time step.[55,58] We used the canonical (NVT) ensemble with a Nosé−Hoover thermostat[61] at 300 K. During the molecular dynamics simulation no symmetry constraints were imposed, and the unit cell was allowed to vary; therefore, each molecule inside the unit cell behaves independently, and they were labeled as A, B, C, and D, as shown in Figure 1.

Classical Molecular Dynamics Simulations. Classical molecular dynamics simulations were carried out in the NPT ensemble with the GROMACS4[62] simulation software. Simulations were carried out using periodic boundary conditions, and the simulation box was constructed by replicating the crystal unit cell five times in the z direction. Interactions between atoms in the simulation cell were described by the OPLS all-atom force field.[63,64] Electrostatic interactions were calculated with a cutoff length of 1.0 nm; long-range electrostatic interactions were computed with the particle-mesh Ewald[65,66] method with 0.12 nm grid spacing and fourth-order B-spline interpolation. Short-range repulsive and attractive dispersion interactions were described by a Lennard-Jones portential, using a cutoff length of 1.0 nm. Tha P-LINCS[67] algorithm was used to constrain bond lengths and angles using a time step of 2 fs. The simulation temperature was maintained at 300 K by weakly coupling the peptides to an external bath using a velocity-scaling thermostat.[68] To keep the pressure in the simulation box at 1 atm, the system was weakly coupled to a Berendsen barostat.[69] Structures were saved for analysis with a frequency of 10 ps.

(51) Markley, J. L.; Bax, A.; Arata, Y.; Hilbers, C. W.; Kaptein, R.; Sykes, B. D.; Wright, P. E.; Wuthrich, K. *Pure Appl. Chem.* **1998**, *70*, 117–142.
(52) Harris, R. K.; Becker, E. D.; Cabral de Menezes, S. M.; Goodfellow, R.; Granger, P. *Solid State Nucl. Magn. Reson.* **2002**, *22*, 458–483.
(53) Morcombe, C. R.; Zilm, K. W. *J. Magn. Reson.* **2003**, *162*, 479–486.
(54) Rienstra, C. M.; Hohwy, M.; Hong, M.; Griffin, R. G. *J. Am. Chem. Soc.* **2000**, *122*, 10979–10990.
(55) Payne, M. C.; Teter, M. P.; Allan, D. C.; Arias, T. A.; Joannopoulos, J. D. *Rev. Mod. Phys.* **1992**, *64*, 1045–1097.
(56) Perdew, J. P.; Burke, K.; Ernzerhof, M. *Phys. Rev. Lett.* **1996**, *77*, 3865–3868.
(57) Yates, J. R.; Pham, T. N.; Pickard, C. J.; Mauri, F.; Amado, A. M.; Gil, A. M.; Brown, S. P. *J. Am. Chem. Soc.* **2005**, *127*, 10216.
(58) Segall, M. D.; Lindan, P. L. D.; Probert, M. J.; Pickard, C. J.; Hasnip, P. J.; Clark, S. J.; Payne, M. C. *J. Phys.: Condens. Matter* **2002**, *14*, 2717–2743.
(59) Clark, S. J.; Segall, M. D.; Pickard, C. J.; Hasnip, P. J.; Probert, M. J.; Refson, K.; Payne, M. C. *Z. Kristallogr.* **2005**, *220*, 567–570.
(60) Vanderbilt, D. *Phys. Rev. B* **1990**, *41*, 7892–7895.
(61) Tuckerman, M. E.; Liu, Y.; Ciccotti, G.; Martyna, G. J. *J. Chem. Phys.* **2001**, *115*, 1678–1702.
(62) Hess, B.; Kutzner, C.; van der Spoel, D.; Lindahl, E. *J. Chem. Theory Comput.* **2008**, *4*, 435–447.
(63) Jorgensen, W. L.; Maxwell, D. S.; TiradoRives, J. *J. Am. Chem. Soc.* **1996**, *118*, 11225–11236.
(64) Kaminski, G. A.; Friesner, R. A.; Tirado-Rives, J.; Jorgensen, W. L. *J. Phys. Chem. B* **2001**, *105*, 6474–6487.
(65) Darden, T. A.; York, D. M.; Pedersen, L. *J. Chem. Phys.* **1993**, *98*, 10089–10092.
(66) van der Spoel, D.; Lindahl, E.; Hess, B.; Groenhof, G.; Mark, A. E.; Berendsen, H. *J. Comput. Chem.* **2005**, *26*, 1701–1718.
(67) Hess, B. *J. Chem. Theory Comput.* **2008**, *4*, 116–122.
(68) Bussi, G.; Donadio, D.; Parrinello, M. *J. Chem. Phys.* **2007**, *126*, 014101+.
(69) Berendsen, H. J. C.; Postma, J. P. M.; van Gunsteren, W. F.; DiNola, A.; Haak, J. R. *J. Chem. Phys.* **1984**, *81*, 3684–3690.

Table 1. Comparison between the Backbone ϕ and ψ Dihedral Angles in the Unit Cell in the PR and TR Structures of the MLF Peptide

	ψ		ϕ		
	Leu	Met	Phe	Leu	Met
PR	−49.3°	151.3°	−155.6°	−67.5°	−146.0°
TR	− 50.4°	157.2°	− 150.4°	−75.4°	−145.8°

Four independent simulations, two of 500 ns and two of 2 μs, were carried out after energy minimization and a short (1 ns) equilibration of the crystal structure. The overall length of the cumulated trajectory is 5 μs, leading to an extensive sampling of the configurational space of the MLF peptide. By analyzing these trajectories we identified a set of four side-chain dihedral angles (χ_1 and χ_3 of methionine and χ_1 and χ_2 of leucine) that undergo the largest number of rotameric transitions. By using these dihedral angles for structure classification, we obtained a list of the 10 most populated conformers of the MLF peptide and their associated statistical weights (Table S2, Supporting Information); these conformers covered more than 90% of all the structures observed during the simulations. A representative structure of each of the 10 states was then chosen for the chemical shift calculations. In order to verify the significance of the statistical weights of the 10 conformers selected, we carried out a further 350 ns molecular dynamics simulation using the AMBER99SB force field;[70] this simulation resulted in the same 10 most populated conformers, although with slightly different statistical weights.

NMR Chemical Shieldings. NMR chemical shieldings were calculated with the gauge including projector augmented wave method (GIPAW).[71] The calculations used Troullier−Martins[72] norm-conserving pseudopotential and plane waves up to a maximum energy of 70 Ry. The integral over the Brillouin zone was sampled at the (1/4,1/4,1/4) point. Since a first-principles calculation gives the absolute chemical shielding tensor, $\vec{\sigma}(r)$, in order to compare the calculated isotropic chemical shielding, $\sigma_{iso}(r) = Tr[\vec{\sigma}(r)]/3$, to the isotropic chemical shift measured in an NMR experiment we referenced the calculated values as $\delta_{iso} = -[\sigma - \sigma_{ref}]$, where the value $\sigma_{ref} = 169.5$ ppm was taken from an earlier work on molecular crystals.[73] In our calculations we neglected quantum zero-point vibrational effects by assuming that they are of the same order of magnitude (0.5 ppm[74]) as in the reference compound.

Results

Relaxation of the Structure. We generated a "totally relaxed" (TR) structure by performing a geometry optimization starting with the "proton-relaxed" (PR) structure of the MLF peptide and allowing all the atoms and the unit cell parameters to relax while keeping the group symmetry fixed; after relaxation the new unit-cell parameters were $a = 21.949$ Å, $b = 22.146$ Å, $c = 5.195$ Å. For comparison the parameters before the minimization were $a = 21.727$ Å, $b = 21.836$ Å, $c = 5.133$ Å; we verified that the α, β, and γ parameters did not change significantly. The most significant conformational changes between the PR and the TR configurations were found along the peptide backbone. In order to compare these structural changes we report in Table 1 the ϕ and ψ torsion angles of the three amino acids inside the unit cell of the MLF crystal; we found small differences of up to 6° (for ψ in Met). The corresponding ^{13}C chemical shifts changes upon relaxation of the crystal structure are presented in Table 2. The major differences (about 5 ppm) are observed in the carbonyl carbon for both Met (C-6) and Phe (C-21) residues.

Time Averaging on the Picosecond Time Scale. In order to analyze the effects of time averaging on the picosecond time scale on the chemical shieldings we generated an *ab initio* molecular dynamics trajectory of 2 ps with a time step of 2 fs. In order to illustrate the fluctuations of the structure that take place during this time, the length of selected covalent bonds along the trajectory is shown in Figure 2; these covalent bonds were found to fluctuate with different amplitudes but a similar period of about 20 fs. The effects of these fluctuations on the calculated chemical shifts are illustrated in Figure 3 for C_α atoms. The time series of the $^{13}C_\alpha$ chemical shifts are shown for Met (Figure 3a), Leu (Figure 3b), and Phe (Figure 3c). Our results show that there are significant fluctuations in the C_α chemical shifts (up to 20 ppm), which take place with a similar period of that of the bond length vibration, but also that the effects of these fluctuations are averaged out within 200 fs, as can be inferred from the convergence of the overall average values of the chemical shifts presented in Figure 3d. The resulting time-averaged chemical shieldings are reported in Table 2.

For reference, we also calculated the chemical shift anisotropy components δ_{11}, δ_{22}, and δ_{33} (Table S1, Supporting Information), which represent the main components of the symmetric part of the diagonalized chemical shielding tensor. The orientation of these three components is determined by the electronic structure of the molecule, therefore offering, at least in principle, information about the molecular structure of the MLF peptide.

Comparison of the Behavior of the Four MLF Molecules in the Unit Cell. The results of the *ab initio* molecular dynamics simulations that we carried out indicate that there are sizable differences in the instantaneous chemical shifts of the four MLF molecules present in the unit cell of the crystal, but also that the time averages of the chemical shifts of equivalent atoms are very similar. For example, the average chemical shift values of the C_α atoms of the four Phe residues in the unit cell are all within 1.1 ppm, with individual standard deviations of about 4 ppm (Figures 3 and 4). These results show that the four different molecules present in the unit cell of the crystal explore similar regions of the conformational space and, therefore, that the simulations that we have carried out are sufficiently converged to allow chemical shifts to be computed with confidence.

Crystal Packing. In order to estimate the effects of crystal packing and long-range interactions on the chemical shifts calculations we extracted a series of conformations of a single MLF molecule at 50 fs intervals from the 2 ps *ab initio* molecular dynamics trajectory of the crystal structure, calculated the time-averaged chemical shifts, and compared them with those calculated for the same molecule in the intact crystal (Figure 5). The chemical environment of every amino acid can be accurately represented by considering the four molecules inside the unit cell, and since intermolecular interactions in the solid state are absent in the isolated molecule, by carrying out this comparison we determined which chemical shifts of the peptide are most affected by intermolecular interactions. The results indicate that crystal packing can modify substantially the average chemical shifts. For example, the chemical shift of Leu-carbonyl C-12 (Figure 5b) is altered by 3.6 ppm since the crystal packing involves the presence of hydrogen bonds between carbonyl carbon atoms and amide groups in the

(70) Hornak, V.; Abel, R.; Okur, A.; Strockbine, B.; Roitberg, A.; Simmerling, C. *Proteins* **2006**, *65*, 712–725.
(71) Pickard, C. J.; Mauri, F. *Phys. Rev. B* **2001**, *6324*, 245101.
(72) Troullier, N.; Martins, J. L. *Phys. Rev. B* **1991**, *43*, 1993–2006.
(73) Gervais, C.; Dupree, R.; Pike, K. J.; Bonhomme, C.; Profeta, M.; Pickard, C. J.; Mauri, F. *J. Phys. Chem. A* **2005**, *109*, 6960–6969.
(74) Vaara, J.; Lounila, K.; Ruud, T.; Helgaker, T. *J. Chem. Phys.* **1998**, *109*, 8388.

Table 2. Comparison between the Experimental and Calculated Chemical Shifts for the MLF Peptide[a]

amino acid	atom type	atom ref	EXP	ΔPR	ΔTR	ΔMD	ΔcMD	BMRB	BMRB SD
Met	C in Nter-COH	1	162.1	3.7	2.0	0.1	−0.8		
Met	C^{α}	2	53.0	4.2	6.0	3.3	1.0	56.2	2.3
Met	C^{β}	3	41.0	3.5	4.8	4.4	−0.7	33.1	2.8
Met	C^{γ}	4	32.8	0.0	3.5	2.6	0.9	32.1	2.2
Met	C^{ε}	5	16.4	4.8	5.0	2.5	0.0	17.4	3.6
Met	C^{O}	6	175.8	6.3	1.0	0.4	0.0	176.2	4.2
Leu	C^{α}	7	59.4	2.8	5.3	3.1	2.7	55.6	2.2
Leu	C^{β}	8	41.0	3.2	5.1	3.4	2.5	42.3	2.3
Leu	C^{δ_1}	10	26.9	5.5	6.3	6.0	4.9	24.7	2.6
Leu	C^{δ_2}	11	20.9	8.9	9.1	8.4	7.1	24.2	2.6
Leu	C^{O}	12	177.6	0.5	−0.3	−1.9	−3.6	177.0	2.1
Phe	C^{α}	13	55.7	1.5	3.9	2.6	−0.8	58.1	2.7
Phe	C^{β}	14	37.2	2.8	4.1	2.2	2.5	39.9	2.7
Phe	C^{γ}	15	139.0	−2.6	1.4	−0.5	−2.6	137.3	18.7
Phe	C^{δ_1}	16	132.0*	3.8	1.8	−0.2	0.1	130.9	6.2
Phe	C^{ε_1}	17	130.4*	3.9	2.6	1.2	−6.0	129.9	6.7
Phe	C^{ζ}	18	129.8*	1.4	0.3	−2.6	−1.7	128.5	6.9
Phe	C^{ε_2}	19	131.3*	2.2	0.8	−1.2	−0.8	130.0	6.6
Phe	C^{δ_2}	20	134.0*	−0.4	2.3	−1.7	−0.1	130.9	5.8
Phe	C^{O}	21	175.0	1.3	−4.2	−3.9	−5.9	175.5	2.4
Phe	C in Cter-Me	22	55.7	3.6	4.5	2.9	1.7		
	rmsd (ppm)			3.3	3.8	4.2	3.0		

[a] (EXP) experimental ^{13}C chemical shifts; (PR) chemical shifts from the proton relaxed structure; (TR) chemical shifts from the totally relaxed structure; (MD) chemical shifts averaged over conformations obtained from a 2 ps first-principles molecular dynamics simulation; (cMD) chemical shifts averaged over conformations obtained from 5μs classical molecular dynamics simulations; Δ represents the difference between EXP and calculated chemical shifts. Average (BMRB) and standard deviation (BMRB SD) values for each atom type are reported from the BMRB (http://www.bmrb.wisc.edu/) database. Chemical shifts of aromatic carbon atoms of Phe that were not assigned are indicated by a *. The average RMSD (in ppm) between the experimental and calculated chemical shifts is reported in the last row.

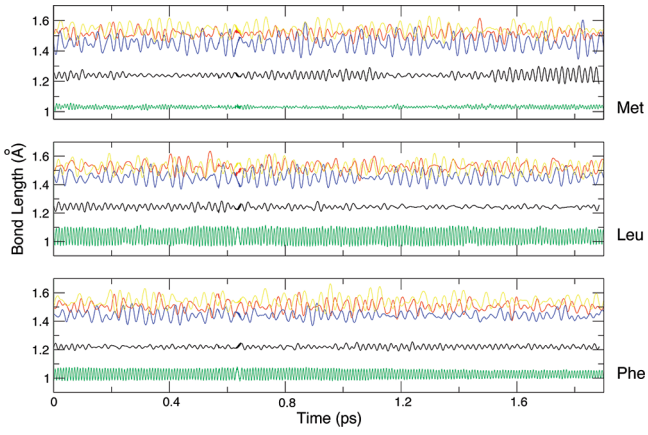

Figure 2. Bond length vibrations during the first-principles molecular dynamics simulations of the MLF peptide carried out in this work: C′ = O (black), C′−C_{α} (red), N−H (green), C_{α}−N (blue), and C_{α}−C_{β} (yellow).

"*c*"direction of the crystal. Other carbon atoms with large differences are (Figure 5c) 3.1 ppm for C-22 (C-terminus of the peptide), 2.8 ppm for C-10 (C^{γ}), 2.6 ppm for C-5 (C^{γ} in Met), 2.4 ppm for C-16 (aromatic ring), and 2.0 ppm for C-1 (formyl terminus). These differences can be also understood from the crystal configuration visualized in Figure 1, which shows crystal packing interactions between C-16 and C-16, and between C-22, C-1, and C-5.

Comparison with Experimental Chemical Shifts. In this work we considered four types of chemical shift calculation (Table 2). In the first (PR), we used the "proton-relaxed" structures, in which the positions of the hydrogen atoms were optimized before the calculation of the chemical shifts. In the second (TR), we used the "totally-relaxed" structures, in which the positions of all the atoms were optimized before the calculations of the chemical shifts. In the third (MD), the chemical shifts were calculated as time-averages over an *ab initio* molecular dynamics trajectory of 2 ps. In the fourth (cMD), the chemical shifts were calculated as time averages over classical molecular dynamics simulations of an overall duration of 5 μs.

The comparison of the four sets of calculated chemical shifts with the experimental ones is presented in Table 2. The accuracy of these calculations is comparable, giving coefficients of correlations between experimental and calculated chemical shifts of 0.9991 (PR), 0.9997 (TR), 0.9997 (MD), and 0.9998 (cMD). The differences obtained between the experimental chemical shifts and the calculated ones, which e.g. in the MD case range from 0.1 ppm to 8.4 ppm and are on average of 3.3 ppm, can be attributed, at least in part, to the intrinsic inaccuracies of current DFT methods. In addition, our results suggest that an averaging over time scales longer than 2 ps is required to estimate the chemical shifts with accuracy. Indeed, chemical shifts are sensitive to dynamics over the millisecond time scale, and it is well-known that protein crystals exhibit significant backbone and side-chain motions over such periods. For example, we observe that the MD chemical shifts of the two Leu C^{δ} atoms are different by 6.0 ppm and 8.4 ppm, respectively, from the corresponding experimental values, suggesting that a rotation of the two methyl groups around the χ_2 angle may be responsible for these differences.

In order to establish whether these differences may be attributed to side-chain dynamics on a time scale longer than 2 ps, which have indeed been observed experimentally in the solid state for the MLF peptide,[50] we carried out classical molecular dynamics (cMD) simulations to generate alternative side-chain rotameric states. By performing an overall sampling of 5 μs we observed that four side-chain dihedral angles (χ_1 and χ_3 of methionine and χ_1 and χ_2 of leucine) exhibited the most significant dynamics. By grouping the conformations generated during the trajectories according to the values of the dihedral angles we identified the 10 most populated rotameric states, which together accounted for over 90% of the conformations (Table S2, Supporting Information). Since the time span of the

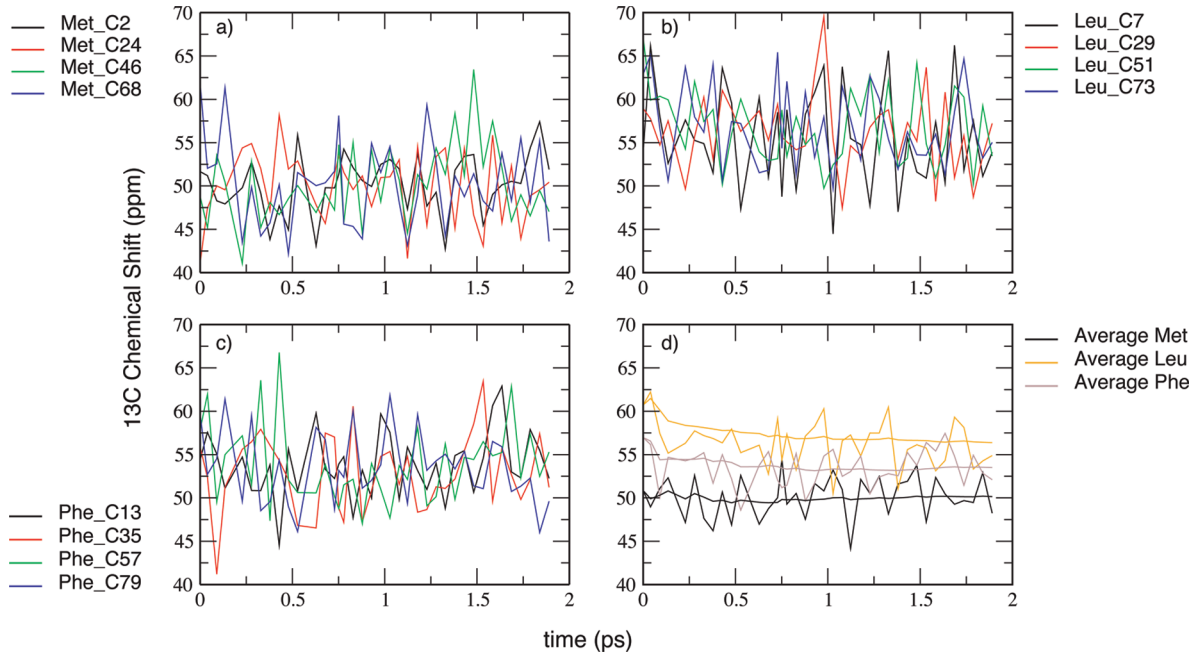

Figure 3. Effects of time-averaging on the ^{13}C chemical shifts of the MLF peptide. (a−c) Time series of the ^{13}C chemical shifts for the four individual molecules in the unit cell; the labeling of the atoms (Leu C51, Phe C79, etc.) refers to correspondent atoms of inequivalent molecules of the simulation cell used. (d) Time series of the average ^{13}C chemical shifts over the four molecules in the unit cell and of the overall average.

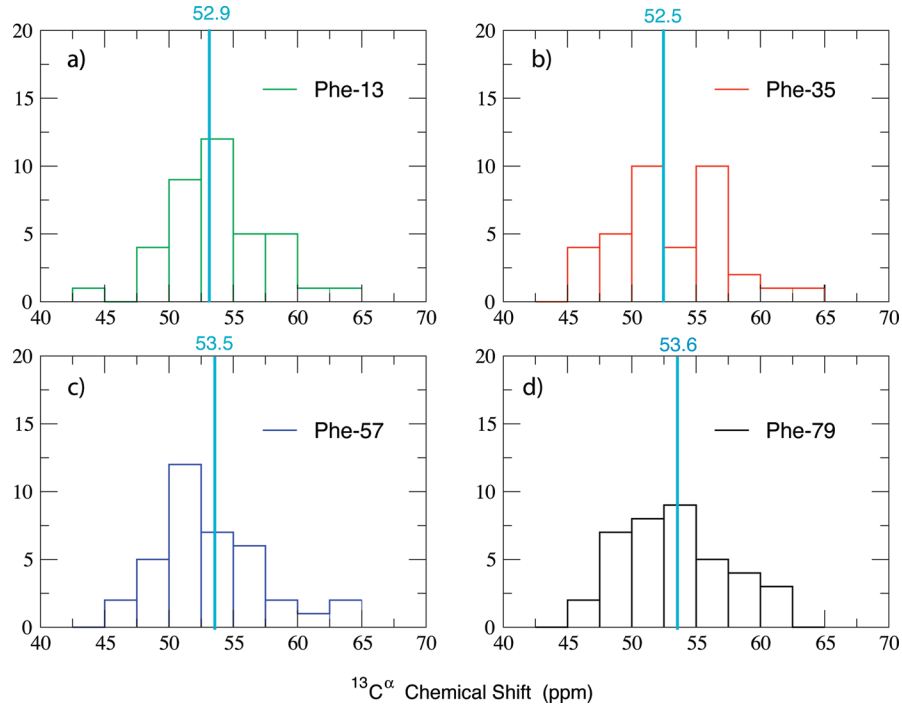

Figure 4. Histograms of the C^{α} chemical shift distributions for the Phe residues of the four MLF molecules in the unit cell (a) Phe-C13, (b) Phe-C35, (c) Phe-C57, (d) Phe-C79. The chemical shifts were calculated for snapshots extracted every 50 fs from a 2 ps trajectory; blue vertical lines indicate the average values.

classical molecular dynamics simulations that we performed allowed us to estimate the statistical weights of each conformer, we selected one representative structure for each of the 10 rotameric states, calculated the corresponding chemical shifts, and averaged their values according to their statistical weights (Table 3 and Table S2, Supporting Information). By following this procedure we reduced the average rmsd to 3.0 ppm. These results provide an initial indication that averaging procedures that take account of the presence of alternative conformers can improve the agreement between the experimental and the calculated chemical shifts.

Although the averaging procedure that we introduced improved the agreement between experimental and calculated chemical shifts in most cases (with 10 C atoms having errors <1 ppm in the cMD case, while only four C atoms have errors <1 ppm in the MD case, see Table 2), for four atoms (Leu $C^{\delta}1$, Leu $C^{\delta 2}$, Phe $C^{\varepsilon 1}$, and Phe C^{O}), the discrepancies were still above

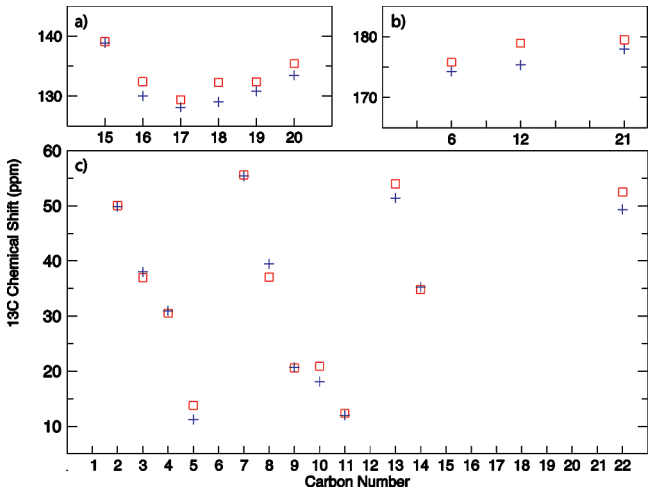

Figure 5. Effects of crystal packing on the chemical shifts of the MLF peptide. We report the comparison between the ^{13}C chemical shifts of an isolated (gas phase, blue pluses) and the corresponding time-averaged values for a molecule in the crystal (red squares) calculated from the simulations that we carried out in this work. Numbering correspond to Figure 1: (a) aromatic carbon atoms; (b) carbonyl carbon atoms; (c) all other carbon atoms.

Table 3. RMSD (in ppm) between Experimental and Calculated Chemical Shifts for the PR and TR Structures, the MD and cMD Averages, and the 10 Representative Structures (S01−S10) Obtained from the Classical Molecular Dynamics Simulations (see also Table S2, Supporting Information)

structure	RMSD
S03	2.6
S07	2.9
S02	2.9
S09	2.9
S10	3.0
S05	3.0
S04	3.0
cMD	3.0
S08	3.1
S06	3.2
S01	3.2
MD	3.3
PR	3.8
TR	4.2

4 ppm. We discuss these cases in order to associate these differences with specific conformational properties.

Leu $C^{\delta 1,2}$**.** The significant dynamics exhibited by Leu $C^{\delta 1}$ and Leu $C^{\delta 2}$ (Figure 6) is associated to large differences between experimental and calculated chemical shifts probably because of a combination of an insufficient sampling of the states considered in the averaging and inaccuracies in the force field used. It is interesting to note that our analysis indicates (Table S2, Supporting Information) that the Leu trans state, which has the largest population in the cMD trajectory (Figure S1, Supporting Information), is associated with higher chemical shift values for Leu $C^{\delta 1}$ and lower ones for Leu $C^{\delta 2}$. By contrast, the Leu gauche$^+$ state has opposite values, i.e. lower chemical shift values for Leu $C^{\delta 1}$ and higher ones for Leu $C^{\delta 2}$.

Phe C^{O}**.** Contrary to Leu $C^{\delta 2}$, Phe C^{O} does not show high mobility (Figure 6). We found that in this case the discrepancy ΔcMD between experimental and calculated chemical shifts is influenced by the conformation of the neighboring Met side chain. We analyzed the distances Met S−Phe O and Met C−Phe

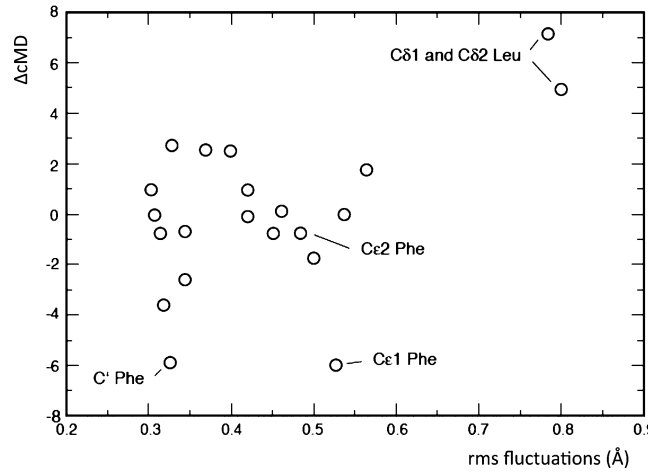

Figure 6. Relationship between the root-mean-square (rms) fluctuations and the difference (ΔcMD) between experimental and calculated (cMD) chemical shifts. The four atoms for which ΔcMD > 4 ppm after the averaging over the classical molecular dynamics trajectory (see Table 2) are indicated.

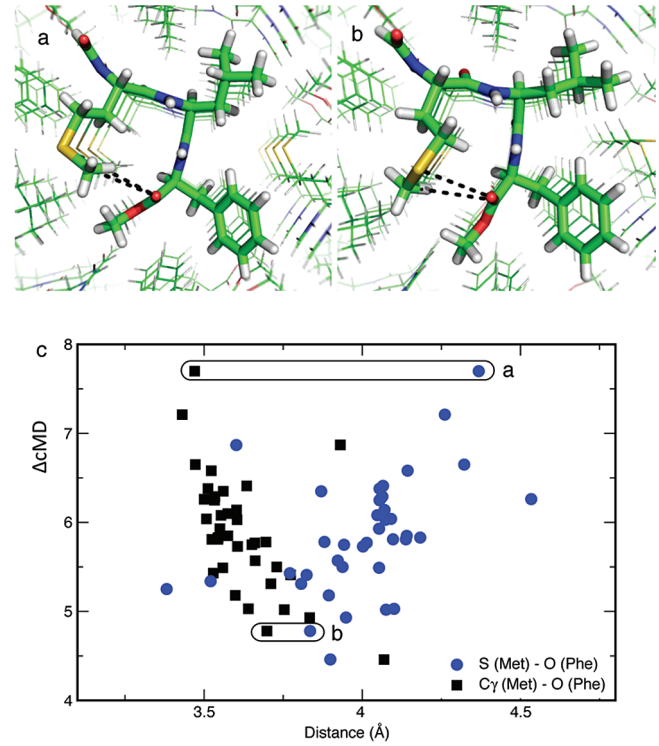

Figure 7. Correlation between the difference (ΔcMD) between experimental and calculated Phe C═O chemical shifts and Met S−Phe O (blue circles) and Met C_γ−Phe O (black squares) distances. (a and b) illustrate the extreme cases highlighted in (c). Data obtained from the four molecules within the unit cell of the 10 most representative structures of the 5 μs cMD trajectory.

O, and found a correlation between them and the chemical shift discrepancy (Figure 7). As noted above, the 5 μs cMD simulations that we carried out can provide only an incomplete description of the dynamics of certain side-chain rotamers. For the Met side chain this seems indeed to be the case; as for Phe C^{O} there is a good agreement between theory and experiment (1.3 ppm) for the proton-relaxed (PR) case.

Phe $C^{\varepsilon 1}$**.** In the case of Phe $C^{\varepsilon 1}$, we initially considered whether the chemical shift discrepancy ΔcMD could be

attributed to $\pi-\pi$ interactions by looking at relative intermolecular distances between two Phe rings in the crystal. However, this interaction is never lost along the cMD trajectory, as distances between the Phe rings remain approximately constant. Similarly, also the consideration of variable ring current contributions using the classical point-dipole model of Pople did not provide significant results. In order to explain the deviations ΔcMD between the calculated chemical shifts and the experimental ones (Table 2), we considered the intermolecular distance $C^{\varepsilon 1}-O$ (C-terminus, AME) (Figure S2), finding that the difference between experimental and calculated chemical shifts tends to zero when this distance approaches 3.2 Å which, however, was outside the range (3.4−4.2 *Å*) sampled during the cMD trajectory (Figure S2, Supporting Information).

Conclusions

We have presented the results of a comparison between experimental and calculated chemical shifts of the MLF peptide in the solid state. In order to investigate the effects of time averaging on the chemical shift values we have used first-principles calculations of the chemical shifts to obtain averages over conformations obtained by first-principles molecular dynamics simulations spanning 2 ps. Our results show that the ^{13}C chemical shifts exhibit large fluctuations of up to 20 ppm, which are averaged out over about 200 fs. We have also presented evidence that the agreement between experimental and calculated chemical shifts can be further improved by averaging over structures obtained from classical molecular dynamics simulations that sample the conformational space explored on the microsecond time scale.

Acknowledgment. We thank Bob Griffin for many discussions. Part of the computational resources were provided by the Cambridge High Performance Computing Service and the Oxford Supercomputer Centre. This work was supported by the Leverhulme Trust, EMBO, and the Royal Society of Chemistry.

Supporting Information Available: Tables S1 and S2. This material is available free of charge via the Internet at http://pubs.acs.org.

JA9062629